# ULTRASONIC IMAGING OF SPALL DAMAGE UNDER REPEATED PLATE IMPACT TESTS WITH C-SCAN ACOUSTIC MICROSCOPE

Koichiro Kawashima, Naoya Nishiura, Makoto Takano
and Osamu Nakayama

Department of Mechanical Engineering
Nagoya Institute of Technology
Nagoya, 466, JAPAN

## INTRODUCTION

Spall damage or fracture is caused by intensive tensile stress pulse within a solid which has been impacted by a high velocity projectile. This damage, microvoids or microcracks distributed within thin layer of the solid, are usually evaluated by destructive means, that is, cutting the samples and observation by SEM or an optical microscope [1-3]. This method requires laborious works. Essentially, with such destructive means we can not monitor the spall damage evolution under repeated impacts on single sample.

With a C-scan acoustic microscope, C-SAM, we can visualize nondestructively internal defects such as voids, cracks, delamination, dissimilar inclusion etc. We have shown on aluminum composites [4] and pure aluminum [5] that the combination of a PVDF focused transducer with a C-SAM were able to visualize the spall damage distribution at arbitrary depth from the impacted surface. By applying this method for repeated plate impact tests, we can monitor nondestructively growth or decrease of the spall damage for single sample under repeated impacts. In this paper, we show the change in spall damage in commercially pure aluminum caused by plate impact test up to three cumulative impacts.

## MECHANISM OF SPALLATION BY PLATE IMPACT TEST

Spall failure is caused by nearly triaxial tensile stress pulse within solid materials. Such tensile stress pulse is generated by the plate impact test in which the target plate is impacted by a flyer plate at high velocity. Figure 1 shows the elastic wave propagation after two plates have collided, under the assumption that both plates have the same mechanical properties and the target plate has double thickness of the flyer. Just after the impact, at time $t_1$, compressive stress waves travel toward the free surfaces of both plates. At the free surface, the phase of the reflected wave is reversed, thus the tensile wave travels back toward the impacted surface with canceling the coming compressive wave as show at time $t_2$. When

*Review of Progress in Quantitative Nondestructive Evaluation, Vol 17*
Edited by D.O. Thompson and D.E. Chimenti, Plenum Press, New York, 1998

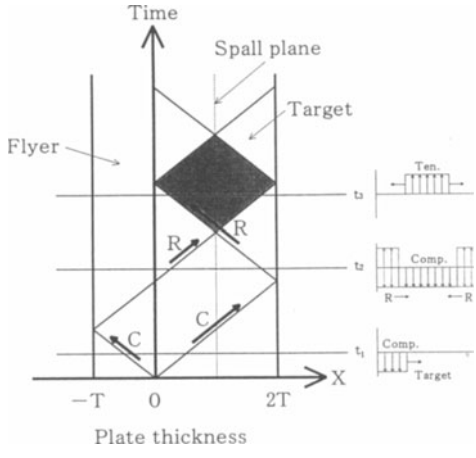


Figure 1. Wave propagation within target and flyer plates.

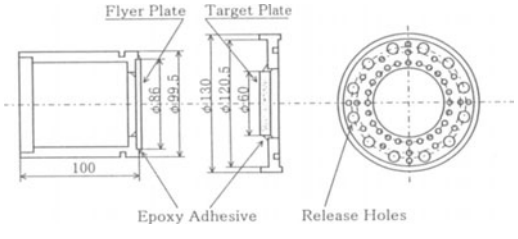


Figure 2. Target and flyer assembly.

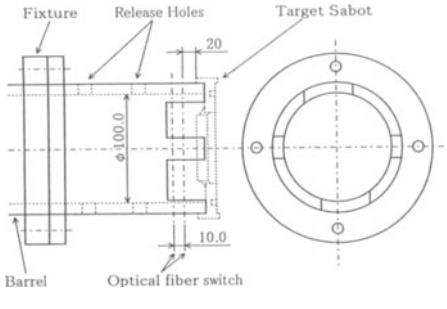


Figure 3. Target holder and velocity measurement unit.

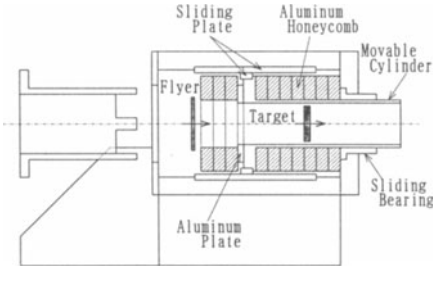


Figure 4. Recovery unit for target plate.

these reflected waves are superposed, at $t_3$, the real tensile stress pulse appears in the shaded domain. When thetensile stress exceeds the spall threshold stress, the spall damage, voids in ductile material or cracks in brittle one, are formed within the target plate. Generally, the spall damage depends on the magnitude as well as duration of the tensile stress pulse. Thus, the damage grows within a thin layer, often called as the spall plane, in which the duration of tensile pulse is longest.

## EXPERIMENTAL METHOD

### Plate Impact Tests

We performed the plate impact test using the target and flyer plates made of commercially pure 1050 aluminum. The flyer plate shown in Fig.2 was accelerated by a single stage gas gun, and its velocity was measured by the optical fiber switches, shown in Fig.3, away 10 and 20mm from the target plate. We have used the target recovery unit, shown in Fig.4, to recover the target. Because the target plate slightly deformed by each impact, it must be machined to a flat circular plate for the next impact. Thus the thickness of the target plate has reduced from the initial 8mm to 5.6mm after the third impact. The thickness of the flyer plate has been kept to an half of the target, thus the spall plane is always in the middle of the plate thickness.

From the measured velocity V, we estimated the compressive stress at the impacted surface by

$$\sigma = \rho C V/2, \quad C = \sqrt{K/\rho} \tag{1}$$

where $\rho$ and K denote the density and bulk modulus of the material.

### B- and C-scan Imaging

The C-scan acoustic microscope used is Olympus UH Pulse-100, of which frequency range, gate width and imaging memory size are 5-200MHz, 20ns-1μs and 640x512(8bit), respectively. A PVDF point-focus transducer was used, of which nominal frequency, diameter and focal length in water are 30MHz, 6.4mm and 25.4mm, respectively. This type of transducer has no focusing rod, therefore it is free from the noise echoes due to reflections at the boundary of the rod. Thus we can visualize defects or voids in samples at arbitrary depth.

We have taken C- and B-scan images of the target plate before and after each impact test. The sample surface was polished by #1500 Emery paper before the imaging. In the following, B- or C-scan images after each impact have been taken under the same imaging condition, i.e., the amplitude gain, gate width, brightness, contrast etc. Thus the change in images results absolutely from the variation of voids due to repeated impacts.

## EXPERIMENTAL RESULTS

### Impact Velocity and Estimated Compressive Stress

Table 1 shows the impact velocity and estimated impact stress for repeated impact. For the sample #32, $\sigma_{3rd}>\sigma_{1st}>\sigma_{2nd}$, whereas for the sample #33 $\sigma_{2nd}>\sigma_{1st}>\sigma_{3rd}$

Table 1. Flyer velocity and impact stress for repeated impacts.

| Sample | Flyer velocity (m/s) | | | Estimated impact stress (GPa) | | |
|---|---|---|---|---|---|---|
| | First | Second | Third | First | Second | Third |
| #32 | 176 | 146 | 186 | 1.3 | 1.0 | 1.3 |
| #33 | 155 | 172 | 104 | 1.1 | 1.2 | 0.74 |
| #34 | 156 | 182 | --- | 1.1 | 1.3 | --- |

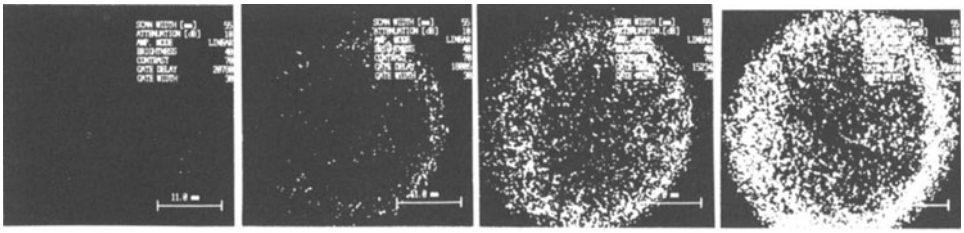


Figure 5. C-scan images of voids distribution at various depth from the impacted surface(#32).

and $\sigma_{2nd}>\sigma_{1st}$ for #34. The spall threshold stress was about 0.8GPa, which is the same of 1100 aluminum.

Dependence of Voids Distribution on Depth from the Impacted Surface

Figure 5 shows C-scan images of voids distribution in the target #32 after the first impact at several depth from the impacted surface. Voids density is highest at depth 4mm, which corresponds to the spall plane shown in Fig.1. We notice some voids at depth 2.5mm, however, most voids appear in the middle layer of 1mm thick. The corresponding B-scan images after the first and second impacts are shown in Fig. 6. Apparently the voids are mainly distributed around the middle of the plate thickness.

Change in Voids Distribution during Repeated Impacts

As shown in Fig.6, after the second impact, most voids in the central portion disappear and new voids appear in the peripheral portion. This means that the voids nucleated by the first impact were compressed and void surfaces were bonded when the second impact stress is lower than the first. Namely a kind of explosive welding [6] has been realized. As shown in later, some threshold stress is required for the bonding of void surfaces.

Figure 7 shows B-scan images of voids after the first, second and third void

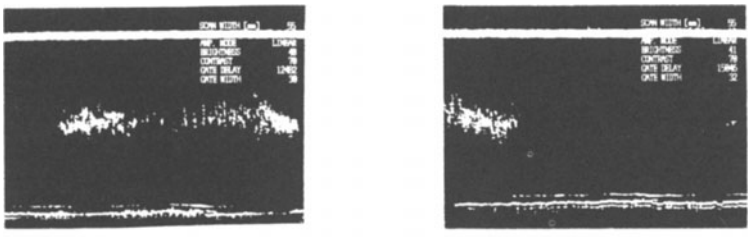

First impact: 1.3GPa Second impact: 1.0GPa

Figure 6. B-scan images of voids after the first and second impacts(#32).

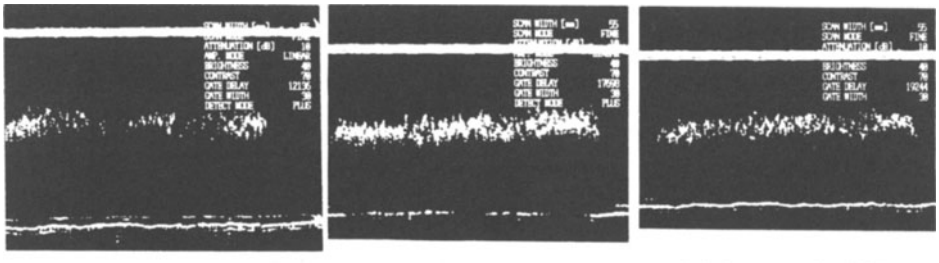

First impact: 1.1GPa Second impact: 1.25GPa Third impact: 0.74GPa

Figure 7. B-scan images of voids after the first,second and third impacts(#33).

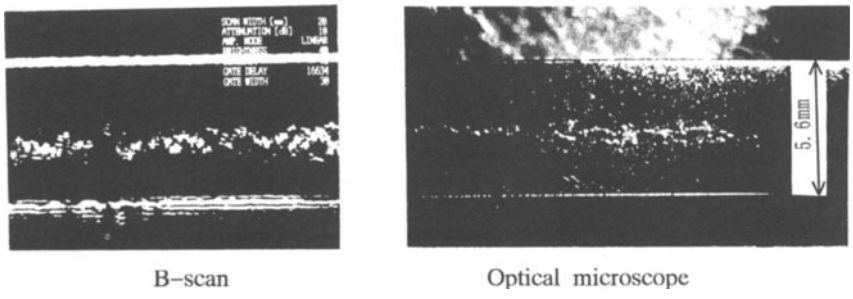


B-scan Optical microscope

Figure 8. Voids distribution observed by B-scan and optical microscope.

density has decreased a little, however it is higher than that caused by the first impacts for the sample #33, where the second impact stress is higher than the first and third. By the second impact, the void density has increased. By the third impact, where the impact stress was 0.74GPa which is slightly lower than the spall threshold stress, the
impact. It is supposed that explosive welding does not activated under some critical stress. Of course, the critical stress may depend on the impact stress history.

The void distribution observed by an optical microscope are compared with the

B-scan image in Fig.8 (a) and (b). These images have been taken at very close cross sections of the sample #34, therefore they may exhibit nearly same damage. The optical image, however, gives less voids than the B-scan image. The difference may result partly from void size visible by an optical microscope, and partly from the imaging mechanism of B-scan. Namely we cannot see voids of micron size by an optical microscope. Moreover, the finite size of the focused beam at focal plane and that of the gate width may cause ghost images for clustered small voids. In addition, the B- and C-scan images of voids appear greater than the actual size, when the void or inclusion is smaller than the ultrasonic beam diameter at the focus [5]. For quantitative evaluation of the spall damage, we should establish the relation between the ultrasonic images of voids and real void size.

## CONCLUSION

The change in spall damage in 1050 aluminum under repeated impacts has been nondestructively monitored by a C-scan acoustic microscope. The growth of spall damage was confirmed when the impact stress had been increased in successive impacts. On the contrary, void surfaces generated by the first impact were bonded when the second impact stress had been lower than the first.

## ACKNOWLEDGEMENT

This work was supported in part by Grant-in-Aid for Scientific Research (A)08555024 from the Ministry of Education, Science, Sports and Culture

## REFERENCES

1.L.Davison and R.A.Graham, Physical Report, 55, 255(1979).
2.M.S.Mayers and C.T.Aimone, Progress in Material Science, 2, 1(1983).
3.D.R.Curran, L.Seaman and D.A.Shockey, Physical Report, 147, 253(1987).
4.K. Kawashima, I.Yuasa and M.Watanabe, in *Metal Matrix Composites*, ed. A.Miravete(Woodhead Publishing, London, 1993) p.234.
5.K.Kawashima, Y.Inamori and N.Nishimura, in *Dynamic Plasticity and Structural Behavior*, eds. S.Tanimura and A.S.Khan(Gordon &Breach Publishing, London, 1995),
p.107.
6.B.Crossland, in *Explosive Welding of Metals and its Applications*, (Oxford Science Publishers, 1982) p.92.